

# On the implied volatility of Asian options under stochastic volatility models

Elisa Alòs\*, Eulalia Nualart\* and Makar Pravosud\*

August 30, 2023

## Abstract

In this paper we study the short-time behavior of the at-the-money implied volatility for arithmetic Asian options with fixed strike price. The asset price is assumed to follow the Black-Scholes model with a general stochastic volatility process. Using techniques of the Malliavin calculus developed in Alòs, García-Lorite and Muguruza [7] we give sufficient conditions on the stochastic volatility in order to compute the level of the implied volatility of the option when the maturity converges to zero. Then, we find a short maturity asymptotic formula for the skew slope of the implied volatility that depends on the correlation between prices and volatilities and the Hurst parameter of the volatility model. We apply our general results to the SABR and fractional Bergomi models, and provide numerical simulations that confirm the accurateness of the asymptotic formulas. Finally, we also apply our results in order to approximate the price of an Asian call option under both stochastic volatility models.

**Keywords:** Stochastic volatility, Asian options, Malliavin calculus, implied volatility

## 1 Introduction

This paper is devoted to the study of Asian call options with payoff of the form

$$\left( \frac{1}{T} \int_0^T S_u du - K \right)_+,$$

where  $T$  denotes the maturity,  $S$  the price of the underlying, and  $K$  the strike of the contract. Asian options of this type are extremely important in energy markets for different reasons. From one hand, typical energy transactions use to take place via multiple deliveries. Then, these transactions are priced on average and not only on a terminal price. Secondly, the payoff is less sensitive to extreme market fluctuations, which becomes interesting in non-liquid markets. Finally, these options tend to be cheaper than the corresponding European vanillas.

The aim of this paper is to study the short-time maturity behavior of the at-the-money implied volatility (ATMIV) of arithmetic Asian options. The study of implied volatility is useful in many ways. Firstly, it can be used to obtain volatilities for pricing OTC options (and other derivatives) with strikes and maturities that are different from

---

\*Universitat Pompeu Fabra and Barcelona School of Economics, Department of Economics and Business, Ramón Trias Fargas 25-27, 08005, Barcelona, Spain. EN acknowledges support from the Spanish MINECO grant PGC2018-101643-B-I00 and Ayudas Fundacion BBVA a Equipos de Investigación Científica 2017.

the ones offered by option exchanges. Secondly, the shape of the implied volatility surface can be used to assess the adequacy of an option pricing model. If the option pricing model is adequate, then it should capture the main properties of the empirical implied volatility surface. In particular, one of the key characteristics of the implied volatility is its skew at the short end and one can easily filter the class of suitable models if the theoretical value of the skew is available for the models of interest. Finally, as one will see further in the paper, one can use implied volatility and its skew to efficiently approximate the option price. Last, but not least, due to the smile effect the hedge ratio has to be adjusted to take into account the market skew. As a result, availability of analytical values of the skew can improve the performance of hedging.

The behavior of the implied volatility for vanilla options has been the object of many works (see for example Lee [12] for a basic introduction to this topic). However, the case of exotic options and more specifically Asian options is less studied and the number of exact analytic results is more limited.

Yang and Ewald [16] compute the implied volatility for OTC traded Asian options under Black-Scholes with constant volatility by combining Monte-Carlo techniques with the Newton method in order to solve nonlinear equations. Approximation methods for pricing Asian options under stochastic volatility models are studied by Forde and Jacquier [9]. Chatterjee et al. [8] develop a Markov chain-based approximation method to price arithmetic Asian options for short maturities under the case of geometric Brownian motion. Fouque and Han [10] generalize the dimension reduction technique of Vecer for pricing arithmetic Asian options. They use the fast mean-reverting stochastic volatility asymptotic analysis to derive an approximation to the option price which takes into account the skew of the implied volatility surface. This approximation is obtained by solving a pair of one-dimensional partial differential equations. The methodology requires the key parameters needed in the PDEs to be estimated from the historical stock prices and the implied volatility surface.

Asymptotics of arithmetic Asian implied volatilities have been studied by Pirjol and Zhu [14] in the case of local volatility. In this paper, the authors make use of large deviations techniques to get accurate approximation formulas for the implied volatility, which are shown to be accurate when compared with the Monte-Carlo simulations. Arithmetic Asian options under the CEV (constant elasticity of variance) model are studied in Pirjol and Zhu [15]. The leading order short maturity limit of the Asian option prices under the CEV model is obtained in closed form. Authors propose an analytic approximation for the Asian options prices which reproduced the exact short maturity asymptotics. Alòs and León [4] compute the short-time level and the skew of the implied volatility of floating strike arithmetic Asian options under the Black-Scholes model with constant volatility by the means of Malliavin calculus.

In this paper, we contribute to the existing literature in several ways. We extend the application of the Malliavin calculus developed in Alòs, García-Lorite and Muguruza [7] by giving general sufficient conditions on a general stochastic volatility model in order to obtain formulas for the short-time limit of the at-the-money level and skew of the implied volatility for Asian options. Moreover, we show how studying Asian option under stochastic volatility reduces to the study of European type options where the underlying is represented by a certain stochastic volatility model, with a modified volatility process which depends on  $T$ . This methodology developed in [7] allows to adapt the results on vanilla options to options on a non lognormal-type distribution and it can also be applied to other European-type exotic options. See for example [7] for an application of this technique to the analysis of the VIX skew. This method is very classical in mathematical finance, for instance, when working with stochastic rates.

To sum up, we study the short-end behavior of the ATMIV of Asian options for local,

stochastic, and fractional volatilities. In particular, we show that

- The short-end limit of the ATMIV is equal to  $\frac{\sigma_0}{3}$ , where  $\sigma_0$  denotes the short-end limit of the spot volatility. See equation (11) in Theorem 1.
- We compute the short-end skew of the ATMIV, which depends on the correlation between prices and stochastic volatility and on the Malliavin derivative of the volatility process, which in the case of fractional volatility models will depend on the Hurst parameter  $H \in (0, 1)$ . See equation (12) in Theorem 1. If prices and volatilities are uncorrelated, the short-end skew is equal to  $\frac{\sqrt{3}\sigma_0}{30}$ . In the case of rough volatilities, that is  $H < \frac{1}{2}$ , we observe in equations (31) and (32) a blow-up that is of the same order as the one we observe in vanilla options (see Alòs et al. [2]).
- We apply the preceding results to the constant volatility case, the SABR model, the fractional Bergomi model, and the local volatility, and perform numerical simulations that confirm the accurateness of the asymptotic formulas. See Section 5. In the case of local volatilities, we verify that our results fit the asymptotic analysis of Pirjol and Zhu [14] and [15].
- Using the short-end limit of the ATMIV and the skew we obtain an analytic approximation of the price of an arithmetic Asian option that we study numerically for the SABR and fractional Bergomi models (see Section 5.5). This is particularly useful for the practitioners since it allows to substitute expensive Monte Carlo simulation and speed up pricing significantly without loss of precision.

The paper is organized as follows: in Section 2 we introduce the main elements of the Malliavin calculus needed through the paper, and the main problem, results and notations. In Section 3 we introduce some preliminary results needed for the proof of the main theorem. In Section 4 we give the proof the main results of the paper. Finally, Section 5 is devoted to the application of the main results to the constant volatility case, the SABR model, the fractional Bergomi model, and the local volatility model, together with some numerical simulations to confirm the accurateness of the asymptotic formulas. We finally use the asymptotic formulas to obtain an analytic approximation of the price of an arithmetic Asian call and we apply it to the SABR and the fractional Bergomi models and compare it with the classical Monte Carlo. The Appendix contains some Malliavin derivatives computations needed through the paper.

## 2 Notations and main results

### 2.1 A primer on Malliavin Calculus

We introduce the elementary notions of the Malliavin calculus used in this paper (see Nualart and Nualart [13]). Let us consider a standard Brownian motion  $Z = (Z_t)_{t \in [0, T]}$  defined on a complete probability space  $(\Omega, \mathcal{F}, \mathbb{P})$  and we denote by  $\mathcal{F}_t$  the filtration generated by  $Z_t$ . Let  $\mathcal{S}^Z$  be the set of random variables of the form

$$F = f(Z(h_1), \dots, Z(h_n)), \quad (1)$$

with  $h_1, \dots, h_n \in L^2([0, T])$ ,  $Z(h_i)$  denotes the Wiener integral of the function  $h_i$ , for  $i = 1, \dots, n$ , and  $f \in C_b^\infty(\mathbb{R}^n)$  (i.e.,  $f$  and all its partial derivatives are bounded). Then the Malliavin derivative of  $F$ ,  $D^Z F$ , is defined as the stochastic process given by

$$D_s^Z F = \sum_{j=1}^n \frac{\partial f}{\partial x_j}(Z(h_1), \dots, Z(h_n)) h_j(s), \quad s \in [0, T].$$

This operator is closable from  $L^p(\Omega)$  to  $L^p(\Omega; L^2([0, T]))$ , for all  $p \geq 1$ , and we denote by  $\mathbb{D}_Z^{1,p}$  the closure of  $\mathcal{S}^Z$  with respect to the norm

$$\|F\|_{1,p} = \left( \mathbb{E} |F|^p + \mathbb{E} \|D^Z F\|_{L^2([0,T])}^p \right)^{1/p}.$$

We also consider the iterated derivatives  $D^{Z,n}$  for all integers  $n > 1$  whose domains will be denoted by  $\mathbb{D}_Z^{n,p}$ , for all  $p \geq 1$ . We will use the notation  $\mathbb{L}_Z^{n,p} := L^p([0, T]; \mathbb{D}_Z^{n,p})$ .

## 2.2 Statement of the problem and main results

We denote by  $(V_t)_{t \in [0, T]}$  the value of a fixed strike arithmetic Asian call option where  $T$  is the maturity. Then, the payoff can be written as

$$V_T = (A_T - K)_+, \quad A_T = \frac{1}{T} \int_0^T S_t dt,$$

where  $(S_t)_{t \in [0, T]}$  is the price of the underlying asset and  $K$  is the fixed strike price.

We assume without loss of generality that the interest rate is equal to zero and we consider the following general stochastic volatility model for the underlying asset price

$$\begin{aligned} dS_t &= \sigma_t S_t dW_t \\ W_t &= \rho W'_t + \sqrt{(1 - \rho^2)} B_t, \end{aligned} \tag{2}$$

where  $S_0 > 0$  is fixed,  $W_t$ ,  $W'_t$ , and  $B_t$  are three standard Brownian motions on  $[0, T]$  defined on the same complete probability space  $(\Omega, \mathcal{G}, \mathbb{P})$ . We assume that  $W'_t$  and  $B_t$  are independent and  $\rho \in [-1, 1]$  is the correlation coefficient between  $W_t$  and  $W'_t$ .

We consider the following assumption on the stochastic volatility of the asset price.

**Hypothesis 1.** *The process  $\sigma = (\sigma_t)_{t \in [0, T]}$  is adapted to the filtration generated by  $W'$ , a.s. positive and continuous, and satisfies that for all  $t \in [0, T]$ ,*

$$c_1 \leq \sigma_t \leq c_2,$$

for some positive constants  $c_1$  and  $c_2$ .

**Remark 1.** *Hypothesis 1 may seem too restrictive since it is not satisfied by the stochastic volatility models considered in Section 5. However, we will show that using a truncation argument, Theorem 1 is still true in all our examples.*

We define the forward price as the martingale  $M_t = \mathbb{E}_t(A_T)$ , where  $\mathbb{E}_t$  denotes the conditional expectation wrt to the filtration  $\mathcal{F}_t$  generated by  $W_t$ . Applying the stochastic Fubini's theorem we get that

$$\begin{aligned} A_T &= \frac{1}{T} \int_0^T S_t dt = \frac{1}{T} \int_0^T \left( S_0 + \int_0^t \sigma_u S_u dW_u \right) dt = \\ &= S_0 + \frac{1}{T} \int_0^T \sigma_u S_u \left( \int_u^T dt \right) dW_u = \\ &= S_0 + \frac{1}{T} \int_0^T (T - u) \sigma_u S_u dW_u, \end{aligned}$$

which implies that

$$dM_t = \frac{\sigma_t S_t (T - t)}{T} dW_t = \phi_t M_t dW_t, \tag{3}$$

where

$$\phi_t := \frac{\sigma_t S_t (T-t)}{TM_t}.$$

Furthermore, the log-forward price  $X_t = \log(M_t)$  satisfies

$$dX_t = \phi_t dW_t - \frac{1}{2} \phi_t^2 dt. \quad (4)$$

**Remark 2.** *One can easily check that Hypothesis 1 implies that  $\phi_t$  is positive a.s. and belongs to  $L^p([0, T] \times \Omega)$ , for all  $p \geq 2$ . In fact, Hypothesis 1 implies that for all  $p \geq 2$ ,  $S_t$  belongs to  $L^p([0, T] \times \Omega)$ ,  $A_T$  belongs to  $L^p(\Omega)$ , and  $M_t^{-1}$  belongs to  $L^p([0, T] \times \Omega)$ .*

**Remark 3.** *Notice that  $\phi_0 = \sigma_0$ . Moreover,*

$$M_t = \frac{1}{T} \left( \int_0^t S_u du + S_t (T-t) \right). \quad (5)$$

*Then,  $TM_t \geq S_t (T-t)$ , and this implies that  $\phi_t \leq \sigma_t$  almost surely.*

The goal of this paper is to study the implied volatility of the Asian call option  $V_t$  which is defined as follows. We denote by  $BS(t, x, k, \sigma)$  the classical Black-Scholes price of a European call with time to maturity  $T-t$ , log-stock price  $x$ , log-strike price  $k$  and volatility  $\sigma$ . That is,

$$BS(t, x, k, \sigma) = e^x N(d_+(k, \sigma)) - e^k N(d_-(k, \sigma)),$$

$$d_{\pm}(k, \sigma) = \frac{x - k}{\sigma \sqrt{T-t}} \pm \frac{\sigma}{2} \sqrt{T-t},$$

where  $N$  is the cumulative distribution function of the standard normal random variable.

Next, we observe that, as  $BS(T, x, k, \sigma) = (e^x - e^k)_+$  for every  $\sigma > 0$ , the price of our Asian call option  $V_t = \mathbb{E}_t(e^{X_T} - e^k)_+$  can be written as

$$V_t = \mathbb{E}_t(BS(T, X_T, k, v_T)), \quad v_t = \sqrt{\frac{1}{T-t} \int_t^T \phi_s^2 ds}. \quad (6)$$

In particular,  $V_T = BS(T, X_T, k, v_T)$ . Then, we define the implied volatility of the option as  $I(t, k) = BS^{-1}(t, X_t, k, V_t)$ , and we denote by  $I(t, k^*)$  the corresponding ATMIV which, in the case of zero interest rates, takes the form  $BS^{-1}(t, X_t, X_t, V_t)$ .

We apply the Malliavin calculus techniques developed in Alòs, García-Lorite and Muguruza [7] in order to obtain formulas for

$$\lim_{T \rightarrow 0} I(0, k^*) \quad \text{and} \quad \lim_{T \rightarrow 0} \partial_k I(0, k^*)$$

under the general stochastic volatility model (2).

In our setting, since we have three Brownian motions  $W, W'$  and  $B$ , if  $h$  is a random variable in  $L^2([0, T])$ , then we have in view of relation (2) that

$$W(h) = \rho W'(h) + \sqrt{1 - \rho^2} B(h).$$

Then, a random variable in  $\mathbb{D}_{W'}^{1,2} \cap \mathbb{D}_B^{1,2}$  is also in  $\mathbb{D}_W^{1,2}$ . In fact, it is easy to see that if  $X$  is a random variable in  $\mathcal{S}^W$ , then

$$D^W X = \rho D^{W'} X + \sqrt{1 - \rho^2} D^B X. \quad (7)$$

Thus, we deduce that for all  $X \in \mathbb{D}_{W'}^{1,2} \cap \mathbb{D}_B^{1,2}$ ,

$$D^W X = \rho D^{W'} X + \sqrt{1 - \rho^2} D^B X. \quad (8)$$

We will need the following additional assumption on the Malliavin differentiability of the stochastic volatility process.

**Hypothesis 2.** For  $p \geq 2$ ,  $\sigma \in \mathbb{L}_{W'}^{2,p}$ .

**Remark 4.** Hypotheses 1 and 2 imply that  $\phi_t$  belongs to  $\mathbb{L}_W^{2,p}$  and  $A_T$  belong to  $\mathbb{D}_W^{2,p}$  for all  $p \geq 2$ . This hypothesis on  $A_T$  corresponds to **(H1)** in Alòs, Garca-Lorite and Muguruza [7].

In order to give the asymptotic skew of the implied volatility as a function of the roughness of the stochastic volatility process we consider the following assumption.

**Hypothesis 3.** There exists  $H \in (0, 1)$  such that for all  $0 \leq s \leq r \leq t \leq T$

$$|D_r^{W'} \sigma_t| \leq M_{r,t}(t-r)^{H-\frac{1}{2}} \quad (9)$$

and

$$|D_s^{W'} D_r^{W'} \sigma_t| \leq N_{s,r,t}(t-r)^{H-\frac{1}{2}}(t-s)^{H-\frac{1}{2}}, \quad (10)$$

where  $M_{r,t}$  and  $N_{s,r,t}$  are positive random variables satisfying for all  $p \geq 1$ ,

$$\mathbb{E}\left(\sup_{0 \leq r \leq t \leq T \leq 1} M_{r,t}^p\right) \leq c_1,$$

and

$$\mathbb{E}\left(\sup_{0 \leq s \leq r \leq t \leq T \leq 1} N_{s,r,t}^p\right) \leq c_2,$$

for some positive constants  $c_1$  and  $c_2$ .

Finally, we will need the following additional assumption on the continuity of the paths of the volatility process.

**Hypothesis 4.** There exists  $\gamma \in (0, H)$  such that for all  $0 \leq s \leq r \leq T \leq 1$

$$|\sigma_r - \sigma_s| \leq K_{r,s}(r-s)^\gamma,$$

where  $K_{r,s}$  is a positive random variable satisfying for all  $p \geq 1$ ,

$$\mathbb{E}\left(\sup_{0 \leq r \leq t \leq T \leq 1} K_{r,s}^p\right) \leq c$$

where  $c > 0$  and  $H$  is the Hurst parameter from Hypothesis 3.

We next provide the the main result of this paper, which is the short-time ATMIV level and skew of an Asian call option under the general volatility model (2).

**Theorem 1.** Assume Hypotheses 1, 2, (9), and 4. Then,

$$\lim_{T \rightarrow 0} I(0, k^*) = \frac{\sigma_0}{\sqrt{3}}. \quad (11)$$

If we further assume (10), then

$$\begin{aligned} & \lim_{T \rightarrow 0} T^{\max(\frac{1}{2}-H, 0)} \partial_k I(0, k^*) \\ &= \lim_{T \rightarrow 0} T^{\max(\frac{1}{2}-H, 0)} \frac{3\sqrt{3}\rho}{\sigma_0 T^5} \int_0^T \left( (T-r) \int_r^T (T-u)^2 \mathbb{E}(D_r^{W'} \sigma_u) du \right) dr \\ & \quad + \lim_{T \rightarrow 0} T^{\max(\frac{1}{2}-H, 0)} \frac{\sqrt{3}\sigma_0}{30}, \end{aligned} \quad (12)$$

and the limit on the right hand side of (12) is finite.

We observe that the level (11) is independent of the correlation  $\rho$  and the Hurst parameter  $H$ , and coincides with the constant volatility case, see Pirjol and Zhu [14] and Alòs and León [4]. Observe also that it coincides with the a.s. limit of  $v_0$ . In fact, by Hypothesis 1 and since  $S_0 = M_0$  we have that a.s.

$$\lim_{T \rightarrow 0} v_0 = \lim_{T \rightarrow 0} \sqrt{\frac{1}{T^3} \int_0^T \frac{\sigma_s^2 S_s^2 (T-s)^2}{M_s^2} ds} = \frac{\sigma_0}{\sqrt{3}}. \quad (13)$$

The skew (12) depends on the correlation parameter  $\rho$  and on the Hurst parameter  $H$ . When prices and volatilities are uncorrelated then the short-time skew equals  $\frac{\sqrt{3}\sigma_0}{30}$ , which again coincides with the constant volatility case, see Pirjol and Zhu [14] and Alòs and León [4]. Observe also that if the term  $\mathbb{E}(D_r^{W'} \sigma_u)$  is of order  $(u-r)^{H-\frac{1}{2}}$  (see Hypothesis 2), then the limit of the right hand side of (12) will be 0 if  $H > 1/2$  and it will converge to a constant when  $H = \frac{1}{2}$ . When  $H < \frac{1}{2}$  we need to multiply by  $T^{\frac{1}{2}-H}$  in order to obtain a finite limit. This is because when  $H > 1/2$ , the fractional Brownian motion is smoother than standard Brownian motion and the effect of the stochastic volatility on the short-time implied volatility will be the same as it was constant, while when  $H < 1/2$ , the fractional Brownian motion is rougher than standard Brownian motion and we obtain the same effect as in the case of vanilla options, see Alòs et al. [2].

The results of Theorem 1 can be used in order to derive an approximation formula for the price of an Asian call option. By definition, the price of the Asian call option writes as

$$V_0 = BS(0, X_0, k, I(0, k))$$

Then, using Taylor's formula we can use the approximation

$$I(0, k) \approx I(0, k^*) + \partial_k I(0, k^*)(k - k^*). \quad (14)$$

The great utility of this relation is that we can use it to approximate the price of an Asian call option for a wide range of stochastic and fractional volatility models. We numerically investigate the quality of this approximation for the SABR and fractional Bergomi models in Section 5.5.

### 3 Preliminary results

We start quoting the two main results obtained in Alòs et al. [7] that will be crucial for the proof of our main Theorem and use the general framework detailed in Section 2.2. The first result is Theorem 6 in Alòs et al. [7] which shows that the short-time limit of the ATMIV equals the short-time limit of the future average of the volatility of the log forward price.

**Theorem 2.** *Assume that for all  $p > 1$ ,  $A_T \in \mathbb{D}_W^{2,p}$ ,  $M_t^{-1} \in L^p([0, T] \times \Omega)$ , and*

$$\lim_{T \rightarrow 0} \mathbb{E} \left( \int_0^T \frac{\Lambda_s}{v_s^2 (T-s)} ds \right) = 0, \quad (15)$$

$$\lim_{T \rightarrow 0} \frac{1}{T^2} \mathbb{E} \left( \frac{1}{v_0} \int_0^T \left( \int_s^T D_s^W \phi_r^2 dr \right)^2 ds \right) = 0, \quad (16)$$

where  $\Lambda_s = \phi_s \int_s^T D_s^W \phi_r^2 dr$ . Then,

$$\lim_{T \rightarrow 0} I(0, k^*) = \lim_{T \rightarrow 0} \mathbb{E}(v_0).$$

The second result is Theorem 8 of Alòs et al. [7] which gives an approximation formula for the short-time limit of the ATMIV skew.

**Theorem 3.** *Assume that for all  $p > 1$ ,  $A_T \in \mathbb{D}_W^{3,p}$ ,  $M_t^{-1} \in L^p([0, T] \times \Omega)$ , hypotheses (15) and (16) are satisfied,*

$$\lim_{T \rightarrow 0} \frac{T^{\max(\frac{1}{2}-H, 0)}}{\sqrt{T}} \mathbb{E} \left( \int_0^T (v_s^2(T-s))^{-3} \Lambda_s \left( \int_s^T \Lambda_r dr \right) ds \right) = 0, \quad (17)$$

$$\lim_{T \rightarrow 0} \frac{T^{\max(\frac{1}{2}-H, 0)}}{\sqrt{T}} \mathbb{E} \left( \int_0^T (v_s^2(T-s))^{-2} \phi_s \left( \int_s^T D_s^W \Lambda_r dr \right) ds \right) = 0, \quad (18)$$

and

$$\lim_{T \rightarrow 0} \frac{T^{\max(\frac{1}{2}-H, 0)}}{T^2} \mathbb{E} \left( \frac{1}{v_0^3} \int_0^T \Lambda_s ds \right) < \infty. \quad (19)$$

Then,

$$\lim_{T \rightarrow 0} T^{\max(\frac{1}{2}-H, 0)} \partial_k I(0, k^*) = \frac{1}{2} \lim_{T \rightarrow 0} \frac{T^{\max(\frac{1}{2}-H, 0)}}{T^2} \mathbb{E} \left( \frac{1}{v_0^3} \int_0^T \Lambda_s ds \right).$$

**Remark 5.** *Observe that there are two typo in Theorem 8 of Alòs et al. [7]. First a factor  $T^{-\gamma}$  missing in their hypothesis **(H5)**. Here we are taking  $\gamma = \min(H - \frac{1}{2}, 0) \in (-\frac{1}{2}, 0]$ . Moreover there is a square missing in the  $u_s(T-s)$  and it should be  $u_s^2(T-s)$ , see for example Lemma 6.3.1 in [6].*

We next present some technical lemmas that will be needed in order to check that the hypotheses of the preceding theorems are satisfied.

**Lemma 1.** *Assume Hypothesis 1. Then, for every  $p \geq 1$ , there exists a constant  $c_p > 0$  such that for all  $0 \leq t < T \leq 1$ ,*

$$\left( \mathbb{E} \left[ v_t^{-2p} \right] \right)^{1/p} \leq c_p \frac{T^2}{(T-t)^2}.$$

*Proof.* We follow a similar idea used in Lemma 3 of [4]. We observe that by the definition of  $\phi_t$  and equation (5), we get that

$$\int_t^T \phi_r^2 dr = \int_t^T \left( \frac{\sigma_r S_r (T-r)}{\int_0^r S_u du + S_r (T-r)} \right)^2.$$

Then, using Hypothesis 1 we get that

$$\int_t^T \phi_r^2 dr \geq c_1^2 \exp \left( -4 \sup_{t \in [0, T]} \left| \int_0^t \sigma_s dW_s - \frac{1}{2} \int_0^t \sigma_s^2 ds \right| \right) \frac{(T-t)^3}{3T^2}.$$

Thus, using again Hypothesis 1,

$$\left( \int_t^T \phi_r^2 dr \right)^{-p} \leq c_1^{-2p} e^{2pTc_2^2} \exp \left( 4p \sup_{t \in [0, T]} \left| \int_0^t \sigma_s dW_s \right| \right) \frac{3^p T^{2p}}{(T-t)^{3p}}. \quad (20)$$

By Burkholder-Davis-Gundy inequality and Hypothesis 1, for any integer  $n \geq 1$ ,

$$\mathbb{E} \left( \sup_{t \in [0, T]} \left| \int_0^t \sigma_s dW_s \right|^n \right) \leq C n^{n/2} (cT)^{n/2},$$

for some positive constants  $c, C$ . Therefore, for  $T \leq 1$ ,

$$\mathbb{E} \exp \left( 4p \sup_{t \in [0, T]} \left| \int_0^t \sigma_s dW_s \right| \right) \leq C \sum_{n=1}^{\infty} \frac{(cn)^{n/2}}{n!}, \quad (21)$$

which is a convergent series. This completes the proof.  $\square$

**Lemma 2.** *Assume Hypothesis 1. Then, for any  $p \geq 1$  there exists a constant  $c_p > 0$  such that for all  $0 \leq t \leq T \leq 1$ ,*

$$\mathbb{E}(M_t^{-p}) \leq c_p.$$

*Proof.* Using (5) and a similar argument as in the proof of Lemma 1, we get that

$$\mathbb{E}(M_t^{-p}) \leq e^{pTc_2^2} \mathbb{E} \exp \left( p \sup_{t \in [0, T]} \left| \int_0^t \sigma_s dW_s \right| \right),$$

and the result follows from (21).  $\square$

Next, we obtain approximation formulas for  $\phi$  and its Malliavin derivative.

**Lemma 3.** *Under Hypotheses 1,2, (9), and 4 the following holds for all  $0 \leq s \leq r \leq T$ ,*

$$\phi_r = \frac{\sigma_0(T-r)}{T} + X_r^1, \quad (22)$$

$$\phi_r^2 = \frac{\sigma_0^2(T-r)^2}{T^2} + X_r^2, \quad (23)$$

$$D_s^W \phi_r = \frac{\rho(T-r)D_s^{W'} \sigma_r}{T} + \frac{(T-r)\sigma_0^2}{T} - \frac{(T-r)(T-s)\sigma_0^2}{T^2} + X_{T,r,s}^3, \quad (24)$$

$$D_s^W \phi_r^2 = \frac{2\sigma_0\rho(T-r)^2 D_s^{W'} \sigma_r}{T^2} + \frac{2(T-r)^2 \sigma_0^3}{T^2} - \frac{2(T-r)^2(T-s)\sigma_0^3}{T^3} + X_{r,s}^4, \quad (25)$$

where  $X^i$  are random variables satisfying for all  $0 \leq s \leq r \leq T \leq 1$ ,

$$\begin{aligned} |X_r^1| &\leq Y_r^1 \frac{(T-r)r^\gamma}{T}, \\ |X_r^2| &\leq Y_r^2 \frac{(T-r)^2 r^\gamma}{T^2}, \\ |X_{r,s}^3| &\leq Y_{r,s}^3 \frac{(T-r)(r-s)^H}{T}, \\ |X_{r,s}^4| &\leq Y_{r,s}^4 \frac{(T-r)^2 r^\gamma (r-s)^H}{T^2}, \end{aligned}$$

and  $Y^i$  are positive random variables satisfying for all  $p \geq 1$

$$\mathbb{E} \left( \sup_{0 \leq s \leq r \leq T \leq 1} |Y_{r,s}^i|^p \right) \leq c_i$$

for some positive constants  $c_i$  only dependent on  $p$  and  $\gamma > 0$  is from Hypothesis 4.

*Proof.* We start proving the decomposition for  $\phi_r$ . We consider the function

$$F(S_s, M_s) := \frac{\sigma_0 S_s (T-r)}{T M_s}, \quad 0 \leq s \leq r.$$

Observe that

$$\phi_r = F(S_r, M_r) + (\sigma_r - \sigma_0) \frac{S_r (T-r)}{T M_r}.$$

Then, using Itô's lemma, we get that we get

$$\begin{aligned} F(S_r, M_r) &= \frac{\sigma_0(T-r)}{T} + \frac{(T-r)}{T} \left\{ \int_0^r \frac{\sigma_0}{M_s} dS_s \right. \\ &\quad \left. - \int_0^r \frac{\sigma_0 S_s}{M_s^2} dM_s + \int_0^r \frac{\sigma_0 \sigma_s^2 S_s^3 (T-s)^2}{M_s^3 T^2} ds \right\}. \end{aligned}$$

Then, using Hypotheses 1 and 4 and Lemma 2, we conclude (22). Similarly, we can write

$$\phi_r^2 = F^2(S_r, M_r) + (\sigma_r^2 - \sigma_0^2) \frac{S_r^2(T-r)^2}{T^2 M_r^2}.$$

and applying Itô's formula to the function  $F^2(S_s, M_s)$  to obtain (23).

We next prove (24). Using expression (36) of the Malliavin derivatives computed in the Appendix, we see that the leading terms are equal to

$$\begin{aligned} & \frac{\rho(T-r)S_r D_s^{W'} \sigma_r}{TM_r} + \frac{\rho^2(T-r)\sigma_r S_r \sigma_s}{TM_r} - \frac{\rho^2(T-r)S_r \sigma_r \sigma_s S_s(T-s)}{T^2 M_r^2} \\ & + \frac{(1-\rho^2)(T-r)\sigma_r S_r \sigma_s}{TM_r} - \frac{(1-\rho^2)(T-r)S_r \sigma_r \sigma_s S_s(T-s)}{T^2 M_r^2} \\ & = \frac{\rho(T-r)S_r D_s^{W'} \sigma_r}{TM_r} + \frac{(T-r)\sigma_r S_r \sigma_s}{TM_r} - \frac{(T-r)S_r \sigma_r \sigma_s S_s(T-s)}{T^2 M_r^2}. \end{aligned}$$

Then, applying Itô's formula to the functions  $F(S_s, M_s) = \frac{S_s}{M_s}$  and  $F(S_s, M_s) = \frac{S_s^2}{M_s^2}$  as above, we obtain (24).

Finally, in order to check (25) it suffice to use the formula  $D_s^W \phi_r^2 = 2\phi_r D_s^W \phi_r$  together with (22) and (24). This concludes the proof.  $\square$

## 4 Proof of Theorem 1

### 4.1 Proof of (11) in Theorem 1: ATM implied volatility level

By (13), it suffices to check that the Hypotheses of Theorem 2 hold true. It is easy to check that Hypotheses 1 and 2 imply the first two hypotheses of Theorem 2 (see Remarks 2 and 4).

We next check (15). Using equation (20) and Cauchy-Schwarz inequality we get that

$$\begin{aligned} \mathbb{E} \int_0^T \frac{\Lambda_s}{v_s^2(T-s)} ds & \leq \int_0^T \frac{T^2}{(T-s)^3} \mathbb{E}(X_T | \Lambda_s) ds \\ & \leq \int_0^T \frac{T^2}{(T-s)^3} (\mathbb{E}(X_T^2))^{1/2} (\mathbb{E}(\Lambda_s^2))^{1/2} ds, \end{aligned}$$

where  $X_T = 3c_1^{-2} e^{2Tc_2^2} \exp\left(4 \sup_{t \in [0, T]} \left| \int_0^t \sigma_s dW_s \right| \right)$ .

Next, due to equation (21) we conclude that  $(\mathbb{E}(X_T^2))^{1/2}$  is bounded as  $T \leq 1$ . Since  $\phi_t \leq \sigma_t$ , Cauchy-Schwarz inequality, Lemma 3 and Hypothesis (9) imply that

$$\begin{aligned} \mathbb{E}(\Lambda_s^2) & \leq C(T-s) \int_s^T \mathbb{E}(|D_s^W \phi_r^2|^2) dr \\ & = O\left((T-s) \int_s^T \frac{(T-r)^4}{T^4} (r-s)^{2H-1} dr\right) \\ & = O\left(\frac{(T-s)^{5+2H}}{T^4}\right). \end{aligned}$$

Finally, we conclude that

$$\mathbb{E} \int_0^T \frac{\Lambda_s}{v_s^2(T-s)} ds = O\left(\int_0^T (T-s)^{H-\frac{1}{2}} ds\right) = O\left(T^{H+\frac{1}{2}}\right),$$

which proves (15).

Similarly, in order to check (16), we use Lemma 3 together with Cauchy-Schwarz inequality, to get that

$$\begin{aligned}
& \frac{1}{T^2} \mathbb{E} \left( \frac{1}{v_0} \int_0^T \left( \int_s^T D_s^W \phi_r^2 dr \right)^2 ds \right) \leq \frac{1}{T^2} \int_0^T (T-s) \int_s^T \mathbb{E} \left( (D_s^W \phi_r^2)^2 \right) dr ds \\
& = O \left( \frac{C}{T^2} \int_0^T (T-s) \int_s^T \frac{(T-r)^4}{T^4} (r-s)^{2H-1} dr ds \right) \\
& = O \left( \int_0^T \frac{(T-s)^{5+2H}}{T^6} ds \right) \\
& = O(T^{2H}).
\end{aligned}$$

Thus, condition (16) also holds and the proof is completed.  $\square$

## 4.2 Proof of (12) in Theorem 1: ATM implied volatility skew

We will apply Theorem 3. We start checking hypothesis (17). Using (20), Lemma 3 and Hypothesis (9), we get that

$$\begin{aligned}
& \mathbb{E} \left( \int_0^T \left( \int_s^T \phi_r^2 dr \right)^{-3} \Lambda_s \left( \int_s^T \Lambda_r dr \right) ds \right) \\
& = O \left( \mathbb{E} \left( \int_0^T \frac{X_T T^6}{(T-s)^9} \frac{T-s}{T} \int_s^t \frac{(T-r)^2}{T^2} |D_s^{W'} \sigma_r| dr \int_s^t \frac{T-r}{T} \int_r^T \frac{(T-u)^2}{T^2} |D_r^{W'} \sigma_u| dudr \right) \right) \\
& = O \left( \int_0^T \frac{1}{(T-s)^3} \int_s^t (r-s)^{H-\frac{1}{2}} dr \int_s^t \int_r^T (u-r)^{H-\frac{1}{2}} dudr \right) \\
& = O \left( \int_0^T (T-s)^{2H-1} \right) = O(T^{2H}).
\end{aligned}$$

Thus, as  $\lim_{T \rightarrow 0} \frac{T^{\max(\frac{1}{2}-H, 0)}}{\sqrt{T}} T^{2H} = \lim_{T \rightarrow 0} T^{\max(H, 2H-\frac{1}{2})} = 0$  for all  $H \in (0, 1)$ , we get that (17) holds true for the leading terms of Lemma 3. The other terms can be treated similarly and we conclude that (17) holds true.

We next check (18). By the definition of  $\Lambda_s$ , we have

$$\begin{aligned}
\int_s^T D_s^W \Lambda_r dr &= \int_s^T D_s^W \left( \phi_r \int_r^T D_r^W \phi_u^2 du \right) dr \\
&= \int_s^T \left( (D_s^W \phi_r) \int_r^T D_r^W \phi_u^2 du + \phi_r \int_r^T D_s^W D_r^W \phi_u^2 du \right) dr,
\end{aligned}$$

where

$$D_s^W D_r^W \phi_u^2 = 2(D_s^W \phi_u D_r^W \phi_u + \phi_u D_s^W D_r^W \phi_u).$$

Next, using Lemma 3 and Hypothesis 3, we get that the leading terms are in expectation of order

$$\begin{aligned}
& \int_s^T D_s^W \phi_r \int_r^T D_r^W \phi_u^2 dudr \\
& = O \left( \int_s^T \frac{(T-r)(r-s)^{H-\frac{1}{2}}}{T} \int_r^T \frac{(T-u)^2 (u-r)^{H-\frac{1}{2}}}{T^2} dudr \right) \\
& = O \left( \frac{(T-s)^{4+2H}}{T^3} \right),
\end{aligned}$$

and

$$\begin{aligned}
& \int_s^T D_s^W \phi_r \int_r^T D_r^W \phi_u^2 du dr \\
&= O\left(\int_s^T \frac{(T-r)}{T} \int_r^T \frac{(T-u)^2(u-r)^{H-\frac{1}{2}}(u-s)^{H-\frac{1}{2}}}{T^2} du dr\right) \\
&= O\left(\frac{(T-s)^{4+2H}}{T^3}\right).
\end{aligned}$$

Then, we conclude that the leading terms satisfy that

$$\begin{aligned}
& \mathbb{E}\left(\int_0^T \left(\int_s^T \phi_r^2 dr\right)^{-2} \phi_s \left(\int_s^T D_s^W \Lambda_r dr\right) ds\right) \\
&= O\left(\int_0^T \frac{(T^3)}{(T-s)^5} \frac{(T-s)^{4+2H}}{T^3} ds\right) \\
&= O\left(\int_0^T (T-s)^{2H-1}\right) = O(T^{2H}).
\end{aligned}$$

Following as above this proves (18).

We are left to check hypothesis (19). Similarly as above, we have that

$$\frac{T^{\max(\frac{1}{2}-H,0)}}{T^2} \mathbb{E}\left(\frac{1}{v_0^3} \int_0^T \Lambda_s ds\right) = O(1),$$

and thus the limit is finite. Therefore, all the hypotheses of Theorem 3 are satisfied.

We finally compute the limit of (19) to check that it coincides with (12). Using Lemma 3, we obtain

$$\begin{aligned}
& \lim_{T \rightarrow 0} \frac{1}{T^2} \mathbb{E}\left(\frac{T^{\max(\frac{1}{2}-H,0)}}{v_0^3} \int_0^T \phi_s \left(\int_s^T D_s^W \phi_r^2 dr\right)^2 ds\right) \\
&= \lim_{T \rightarrow 0} \mathbb{E}\left(\frac{T^{\max(\frac{1}{2}-H,0)}}{T^2 v_0^3} \int_0^T \frac{\sigma_0(T-s)}{T} \int_s^T \left(\frac{2\sigma_0 \rho(T-r)^2 D_s^{W'} \sigma_r}{T^2} \right. \right. \\
&\quad \left. \left. + \frac{2(T-r)^2 \sigma_0^3}{T^2} - \frac{2(T-r)^2(T-s)\sigma_0^3}{T^3}\right) dr ds\right) \\
&= \lim_{T \rightarrow 0} \mathbb{E}\left(\frac{2\sigma_0^2 \rho T^{\max(\frac{1}{2}-H,0)}}{T^5 v_0^3} \int_0^T \left((T-s) \int_s^T (T-r)^2 D_s^{W'} \sigma_r dr\right) ds\right) \\
&\quad + \lim_{T \rightarrow 0} T^{\max(\frac{1}{2}-H,0)} \mathbb{E}\left(\frac{\sigma_0^4}{45v_0^3}\right).
\end{aligned}$$

Using (20) and dominated convergence we see that

$$\lim_{T \rightarrow 0} T^{\max(\frac{1}{2}-H,0)} \mathbb{E}\left(\frac{\sigma_0^4}{45v_0^3}\right) = \lim_{T \rightarrow 0} T^{\max(\frac{1}{2}-H,0)} \frac{\sqrt{3}\sigma_0}{60},$$

since  $v_0^2$  converges a.s. towards  $\frac{\sigma_0^2}{3}$  as  $T \rightarrow 0$ . In order to compute the remaining limit we write

$$\begin{aligned}
& \lim_{T \rightarrow 0} \mathbb{E}\left(\frac{2\sigma_0^2 \rho T^{\max(\frac{1}{2}-H,0)}}{T^5 v_0^3} \int_0^T \left((T-s) \int_s^T (T-r)^2 D_s^{W'} \sigma_r dr\right) ds\right) \\
&= \lim_{T \rightarrow 0} \mathbb{E}\left(\left(\frac{1}{v_0^3} - \frac{3\sqrt{3}}{\sigma_0^3}\right) A_T\right) + \lim_{T \rightarrow 0} \frac{3\sqrt{3}}{\sigma_0^3} \mathbb{E}(A_T),
\end{aligned}$$

where

$$A_T = \frac{2\rho\sigma_0^2 T^{\max(\frac{1}{2}-H,0)}}{T^5} \int_0^T \left( (T-s) \int_s^T (T-r)^2 D_s^{W'} \sigma_r dr \right) ds.$$

By dominated convergence we see that

$$\lim_{T \rightarrow 0} \mathbb{E} \left( \left( \frac{1}{v_0^3} - \frac{3\sqrt{3}}{\sigma_0^3} \right) A_T \right) = 0,$$

which concludes the proof of (12).  $\square$

## 5 Numerical analysis

In this section we present numerical evidence of the adequacy of Theorems 1 in different settings.

### 5.1 The Black-Scholes model under constant volatility

We consider the Black-Scholes model (2) under constant volatility  $\sigma > 0$ , that is,

$$dS_t = \sigma S_t dW_t, \quad S_t = S_0 e^{\sigma W_t - \frac{\sigma^2}{2} t}.$$

Appealing to Theorem 1 with  $\rho = 0$  and  $H = \frac{1}{2}$ , we conclude that the level and the skew of the at-the-money implied volatility satisfy that

$$\lim_{T \rightarrow 0} I(0, k^*) = \frac{\sigma}{\sqrt{3}} \quad \text{and} \quad \lim_{T \rightarrow 0} \partial_k I(0, k^*) = \frac{\sigma\sqrt{3}}{30}.$$

Notice that these results coincide with the ones obtained in Pirjol and Zhu [14], see Section 7.2 below.

We next proceed with numerical simulations with parameters

$$S_0 = 10, \quad T = \frac{1}{252}, \quad \sigma \in [0.1, 0.2, \dots, 1.4].$$

We use the control variates method in order to get estimates of an Asian call option price. As a control variate we use a geometric Asian call option whose price is given by

$$BS_{GeomAsian} = e^{-\frac{1}{4}\sigma_G^2 T} S_0 N(d_1) - KN(d_2), \quad (26)$$

where

$$d_1 = \frac{\log \frac{S_0}{K} + \frac{1}{4}\sigma_G^2 T}{\sigma_G \sqrt{T}}, \quad d_2 = d_1 - \sigma_G \sqrt{T}, \quad \sigma_G = \frac{\sigma}{\sqrt{3}}.$$

Then, the Asian call option price estimator has the following form

$$\hat{BS}_{Asian} = \frac{1}{N} \sum_{i=1}^N V_T^i - c^* \frac{1}{N} \sum_{i=1}^N (\hat{BS}_{Asian}^i - BS_{GeomAsian}), \quad (27)$$

where

$$c^* = \frac{\sum_{i=1}^N (V_T^i - \frac{1}{N} \sum_{i=1}^N A_T^i) (\hat{BS}_{Asian}^i - BS_{GeomAsian})}{\sum_{i=1}^N (\hat{BS}_{Asian}^i - BS_{GeomAsian})^2},$$

and

$$\hat{BS}_{Asian}^i = \max(\sqrt{S_0^i S_1^i \dots S_m^i} - K, 0),$$

where  $N = 2000000$ ,  $m = 50$ ,  $V_T^i = \max(A_T^i - K, 0)$  and the sub-index  $i$  indicates the quantity estimated from a realisation of a path from Monte Carlo simulation.

In order to retrieve an estimation for the implied volatility  $\hat{I}(0, k^*)$  from the estimated Asian call price we use the algorithm presented in Jäckel [11]. For the estimation of the skew, we use the following finite difference approximation

$$\partial_k \hat{I}(0, k^*) = \frac{\hat{I}(0, k^* \log(1 + \Delta k)) - \hat{I}(0, \frac{k^*}{\log(1 + \Delta k)})}{2 \log(1 + \Delta k)}, \quad (28)$$

where  $\Delta k = 0.001$ .

The at-the-money level and the skew of the implied volatility are presented at Figure 1. We conclude that the results of the numerical simulation are in line with the presented theoretical formulas.

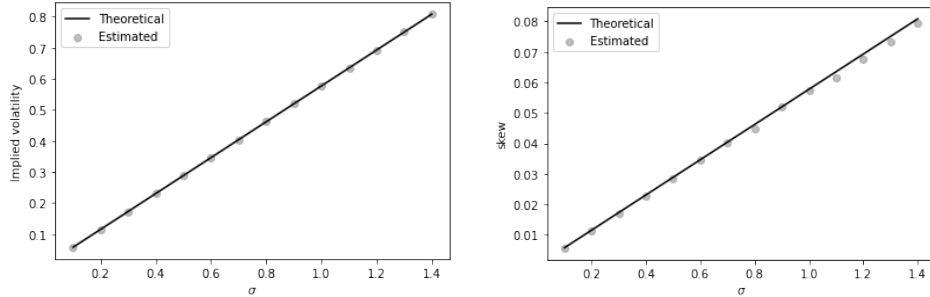


Figure 1: At-the-money level and skew of the IV under Black-Scholes

## 5.2 The SABR model

In this section we consider the SABR stochastic volatility model with skewness parameter 1, which is the most common case from a practical point of view. This corresponds to equation (2), where  $S_t$  denotes the forward price of the underlying asset and

$$d\sigma_t = \alpha \sigma_t dW'_t, \quad \sigma_t = \sigma_0 e^{\alpha W'_t - \frac{\alpha^2}{2} t}.$$

where  $\alpha > 0$  is the volatility of volatility.

Notice that this model does not satisfy Hypothesis 1, so a truncation argument similar as in Section 5 in Alòs and Shiraya [5] is needed in order to check that Theorem 1 is true for this model. We define  $\varphi(x) = \sigma_0 \exp(x)$ . For every  $n > 1$ , we consider a function  $\varphi_n \in C_b^2$  satisfying that  $\varphi_n(x) = \varphi(x)$  for any  $x \in [-n, n]$ ,  $\varphi_n(x) \in [\varphi(-2n) \vee \varphi(x), \varphi(-n)]$  for  $x \leq -n$ , and  $\varphi_n(x) \in [\varphi(n), \varphi(x) \wedge \varphi(2n)]$  for  $x \geq n$ . We set

$$\sigma_t^n = \varphi_n \left( \alpha W'_t - \frac{\alpha^2}{2} t \right).$$

It is easy to see that  $\sigma_t^n$  satisfies Hypotheses 1, 2, (9), and 4. In fact, for  $r \leq t$ , we have that

$$D_r^{W'} \sigma_t^n = \varphi'_n \left( \alpha W'_t - \frac{\alpha^2}{2} t \right) \alpha,$$

which implies that (9) holds with  $H = \frac{1}{2}$  and Hypothesis 4 is satisfied with  $\gamma < 1/2$ . Therefore, appealing to Theorem 1 and using the fact that  $\sigma_0^n = \sigma_0$ , we conclude that

$$\lim_{T \rightarrow 0} I^n(0, k^*) = \frac{\sigma_0}{\sqrt{3}}. \quad (29)$$

where  $I^n$  denotes the implied volatility under the volatility process  $\sigma_t^n$ . We then write

$$I(0, k^*) = I^n(0, k^*) + I(0, k^*) - I^n(0, k^*).$$

By the mean value theorem,

$$\begin{aligned} I(0, k^*) - I^n(0, k^*) &= \partial_\sigma(BS^{-1}(0, X_0, X_0, \xi))(V_0 - V_0^n) \\ &= e^{-X_0 + \frac{\xi^2 T}{8}} \frac{\sqrt{2\pi}}{\sqrt{T}} (V_0 - V_0^n), \end{aligned}$$

for some  $\xi \in (V_0, V_0^n)$ , where  $V_0^n$  is the option price under  $\sigma^n$ . Thus, for  $T \leq 1$  and  $n > \alpha^2$ ,

$$\begin{aligned} |I(0, k^*) - I^n(0, k^*)| &\leq \frac{C_n}{\sqrt{T}} \mathbb{E} \left( |e^{X_T} - e^{X_T^n}| \mathbf{1}_{\sup_{s \in [0, T]} |\ln(\sigma_s/\sigma_0)| > n} \right) \\ &\leq \frac{C_n}{\sqrt{T}} \mathbb{E} [ (|e^{X_T} + e^{X_T^n}|^2)^{1/2} ]^{1/2} \left[ \mathbb{P} \left( \sup_{s \in [0, T]} |\ln(\sigma_s/\sigma_0)| > n \right) \right]^{1/2} \\ &\leq \frac{C_n}{\sqrt{T}} \left[ \mathbb{P} \left( \sup_{s \in [0, T]} |\alpha W'_s - \alpha^2 s/2| > n \right) \right]^{1/2} \\ &\leq \frac{C_n}{\sqrt{T}} \left[ \mathbb{P} \left( \sup_{s \in [0, T]} |W_s| > \frac{n}{2\alpha} \right) \right]^{1/2}, \end{aligned}$$

for some constant  $C_n > 0$  that changes from line to line. Then, Markov's inequality implies that for all  $p > 2$ ,

$$|I(0, k^*) - I^n(0, k^*)| \leq \frac{C_n}{\sqrt{T}} \left( \frac{2\alpha}{n} \right)^{p/2} \left[ \mathbb{E} \left( \sup_{s \in [0, T]} |W_s|^p \right) \right]^{1/2} \leq C_n T^{\frac{p}{2} - \frac{1}{2}},$$

Thus, taking  $p > 4$ , we conclude that

$$\lim_{T \rightarrow 0} I(0, k^*) = \frac{\sigma_0}{\sqrt{3}}.$$

On the other hand, for  $s \leq r \leq t$ , we have

$$D_s^{W'} D_r^{W'} \sigma_t^n = \varphi_n'' \left( \alpha W'_t - \frac{\alpha^2}{2} t \right) \alpha^2,$$

which implies that (10) holds with  $H = \frac{1}{2}$ . Therefore, appealing to Theorem 1 we get that

$$\lim_{T \rightarrow 0} \partial_k I^n(0, k^*) = \frac{\sqrt{3}\rho\alpha\varphi_n'(\sigma_0)}{5\sigma_0^n} + \frac{\sqrt{3}\sigma_0^n}{30} = \frac{\sqrt{3}\rho\alpha}{5} + \frac{\sqrt{3}\sigma_0}{30}.$$

Next, similarly as above we can write

$$\partial_k I(0, k^*) = \partial_k I^n(0, k^*) + \partial_k (I(0, k^*) - I^n(0, k^*)).$$

By the mean value theorem,

$$\begin{aligned} \partial_k (I(0, k^*) - I^n(0, k^*)) &= \partial_\sigma \partial_k (BS^{-1}(0, X_0, X_0, \xi))(V_0 - V_0^n) \\ &= -e^{-X_0 + \frac{\xi^2 T}{8}} \frac{\sqrt{2\pi}}{2} \xi (V_0 - V_0^n), \end{aligned}$$

for some  $\xi \in (V_0, V_0^n)$ . Thus, proceeding as above we conclude that

$$\lim_{T \rightarrow 0} \partial_k I(0, k^*) = \frac{\sqrt{3}\rho\alpha}{5} + \frac{\sqrt{3}\sigma_0}{30}.$$

We next proceed with some numerical simulations using the following parameters

$$S_0 = 10, T = \frac{1}{252}, dt = \frac{T}{50}, \alpha = 0.5, \rho = -0.3, \sigma_0 = (0.1, 0.2, \dots, 1.4).$$

In order to get estimates of an Asian call option we use antithetic variates. The estimate of the price is defined as follows

$$\hat{V}_{sabr} = \frac{\frac{1}{N} \sum_{i=1}^N V_T^i + \frac{1}{N} \sum_{i=1}^N V_T^{i,A}}{2}, \quad (30)$$

where  $N = 2000000$  and the sub-index  $A$  denotes the value of an Asian call option computed on the antithetic trajectory of a Monte Carlo path.

We use equation (28) in order to get estimates of the skew. In Figure 2 we present the results of a Monte Carlo simulation which aims to evaluate numerically the level and the skew of the at-the-money implied volatility of an Asian call option under the SABR model. Again, the numerical results fit the theoretical ones.

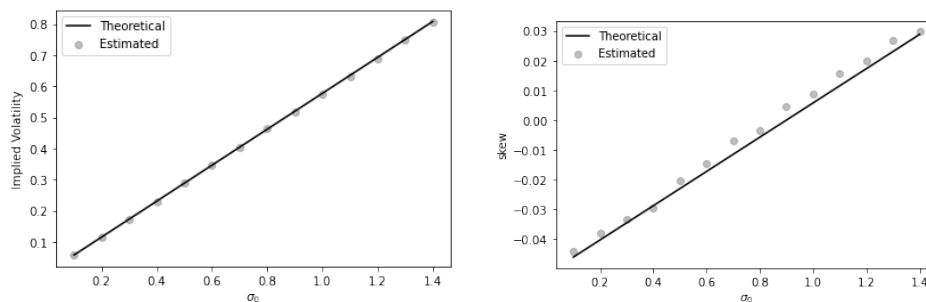


Figure 2: At-the-money level and skew of the IV under SABR model.

### 5.3 The fractional Bergomi model

The fractional Bergomi stochastic volatility model assumes equation (2) with

$$\sigma_t^2 = \sigma_0^2 e^{v\sqrt{2H}Z_t - \frac{1}{2}v^2t^{2H}}, \quad Z_t = \int_0^t (t-s)^{H-\frac{1}{2}} dW_s',$$

where  $H \in (0, 1)$  and  $v > 0$ , see Example 2.5.1 in Alòs and García-Lorite [6].

As for the SABR model, a truncation argument is needed in order to apply Theorem 1, as Hypothesis 1 is not satisfied. We define  $\varphi$  and  $\varphi_n$  as for the SABR model, and we set

$$\sigma_t^n = \varphi_n \left( \frac{1}{2}v\sqrt{2H}Z_t - \frac{1}{4}v^2t^{2H} \right).$$

It is easy to see that  $\sigma_t^n$  satisfies Hypotheses 1, 2, (9), and 4. In fact, for  $r \leq t$ , we have that

$$D_r^{W'} \sigma_t^n = \varphi_n' \left( \frac{1}{2}v\sqrt{2H}Z_t - \frac{1}{4}v^2t^{2H} \right) \frac{1}{2}v\sqrt{2H}(t-r)^{H-\frac{1}{2}},$$

which implies that Hypothesis (9) holds and Hypothesis 4 is satisfied with  $\gamma < H$ . Moreover, for  $s \leq r \leq t$ , we have

$$D_s^{W'} D_r^{W'} \sigma_t^n = \varphi_n'' \left( \frac{1}{2} v \sqrt{2H} Z_t - \frac{1}{4} v^2 t^{2H} \right) \frac{1}{4} v^2 \sqrt{4H^4} (t-r)^{H-\frac{1}{2}} (t-s)^{H-\frac{1}{2}},$$

which implies that (10) holds. Therefore, by Theorem 1 we get that (29) holds. Concerning the short maturity limit of the skew, we observe that

$$\mathbb{E}(D_r^{W'} \sigma_u) = e^{-\frac{1}{8} v^2 u^{2H}} \frac{1}{2} \sigma_0 v \sqrt{2H} (u-r)^{H-\frac{1}{2}}.$$

which gives

$$\lim_{T \rightarrow 0} \partial_k I^n(0, k^*) = \begin{cases} \frac{\sqrt{3}\sigma_0}{30} & \text{if } H > \frac{1}{2} \\ \frac{\sqrt{3}\rho v}{10} + \frac{\sqrt{3}\sigma_0}{30} & \text{if } H = \frac{1}{2}, \end{cases} \quad (31)$$

and for  $H < \frac{1}{2}$

$$\begin{aligned} & \lim_{T \rightarrow 0} T^{\frac{1}{2}-H} \left( \partial_k I^n(0, k^*) - \frac{\sqrt{3}\sigma_0}{30} \right) \\ &= \frac{3\sqrt{6H}\rho v}{(1+H-\frac{1}{2})(2+H-\frac{1}{2})(3+H-\frac{1}{2})(5+H-\frac{1}{2})}. \end{aligned} \quad (32)$$

Finally, similarly as for the SABR model one can easily show that for  $n$  sufficiently large but fixed,

$$\lim_{T \rightarrow 0} (I(0, k^*) - I^n(0, k^*)) = 0$$

and

$$\lim_{T \rightarrow 0} \partial_k (I(0, k^*) - I^n(0, k^*)) = 0,$$

so (29), (31), and (32) are also true for  $I(0, k^*)$ .

The parameters used for the Monte Carlo simulation are the following

$$S_0 = 10, T = 0.001, dt = \frac{T}{50}, H = (0.4, 0.7), v = 0.5, \rho = -0.3, \sigma_0 = (0.1, 0.2, \dots, 1.4).$$

In order to obtain an estimate of the price of an Asian call option under the fractional Bergomi model we use the combination of antithetic and control variates presented in equations (27) and (30). That is, we first sample the process from the Bergomi model and the antithetic analogue. We then average the payoffs calculated from both paths. Finally, use the geometric Asian as control variate assuming constant volatility model at level  $\sigma_0$ .

In Figure 3 we plot the estimates of the level of the ATMIV of the Asian call option and we observe that the result is independent of  $H$  as stated in Theorem 1.

In Figure 4 we simulate the ATMIV skew of the Asian call option as a function of the maturity as well as its least squares fit in order to observe the blow up to  $-\infty$  for the case  $H = 0.4$ .

We then plot the quantities  $T^{\frac{1}{2}-H} \partial_k \hat{I}(0, k^*)$  for  $H = 0.4$  and  $\partial_k \hat{I}(0, k^*)$  for  $H = 0.7$  in Figure 5 as a function of  $\sigma_0$ . For  $H = 0.4$ , the line  $-0.0243 + 0.032\sigma_0$  corresponds to the least square fit while formula (32) gives the line  $-0.0286 + 0.029\sigma_0$ . This difference is due to the numerical instability of the finite difference estimation at short maturity in the presence of rough noise and could be improved by increasing considerably the number of Monte Carlo samples or applying a variance reduction technique. For  $H = 0.7$ , we observe that formula (31) fits well the Monte Carlo estimates.

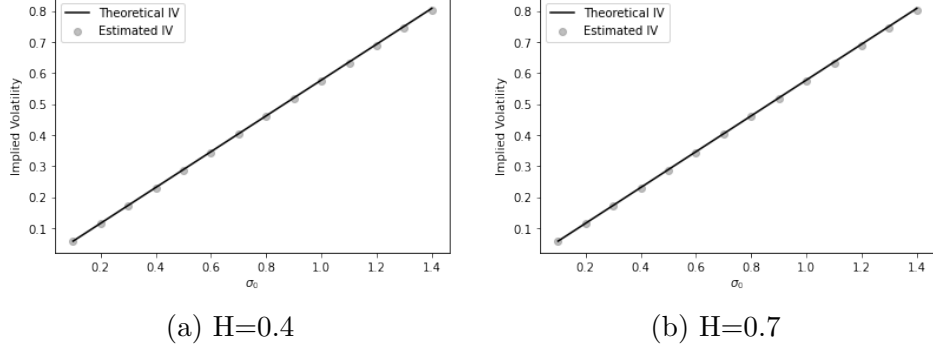


Figure 3: At-the-money level of the IV under fractional Bergomi model

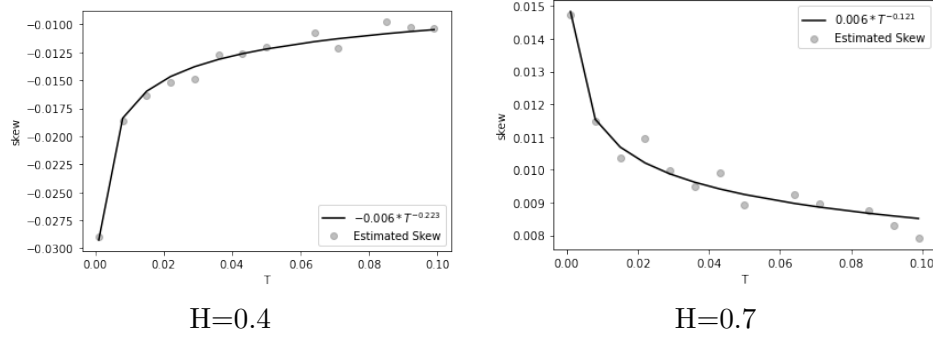


Figure 4: At-the-money IV skew as a function of  $T$  under fractional Bergomi model

#### 5.4 Local volatility model

The short-maturity limit of the ATMIV level and skew of an Asian option under local volatility has already been computed in Pirjol and Zhu [14]. The aim of this section is to check that our Theorem 1 provides the same asymptotics as the ones obtained in that paper. We consider the local volatility model

$$dS_t = \sigma(S_t)S_t dW_t, \quad (33)$$

where  $\sigma(\cdot)$  is a twice differentiable function. In Proposition 19 of Pirjol and Zhu [14] they show that the following expansion holds for  $x = \log(\frac{K}{S_0})$  around the ATM point

$$\lim_{T \rightarrow 0} I(0, k^*) = \frac{\sigma(S_0)}{\sqrt{3}} \left( 1 + \left( \frac{1}{10} + \frac{3\sigma'(S_0)}{5\sigma(S_0)} S_0 \right) x + O(x^2) \right). \quad (34)$$

Then, differentiating equation (34), we obtain that

$$\lim_{T \rightarrow 0} \partial_k I(0, k^*) = \frac{1}{\sqrt{3}} \left( \frac{1}{10} \sigma(S_0) + \frac{3}{5} S_0 \sigma'(S_0) \right). \quad (35)$$

We next apply Theorem 1 in the case of the local volatility model (33) with  $\sigma_t = \sigma(S_t)$  and  $\rho = 1$  to verify that we obtain the same expressions as in (11) and (35). For the level, we directly see that when  $\sigma(S_t)$  equals  $\sigma_t$  and  $K = S_0$ , (34) coincides with the limit in (11). For the skew, we need to compute  $D_r \sigma(S_t)$ . We have for  $r \leq u$ ,

$$D_r \sigma(S_u) = \sigma'(S_u) D_r(S_u) = \sigma'(S_u) \left( \sigma(S_r) S_r + \int_r^u D_r(\sigma(S_s) S_s) dW_s \right).$$

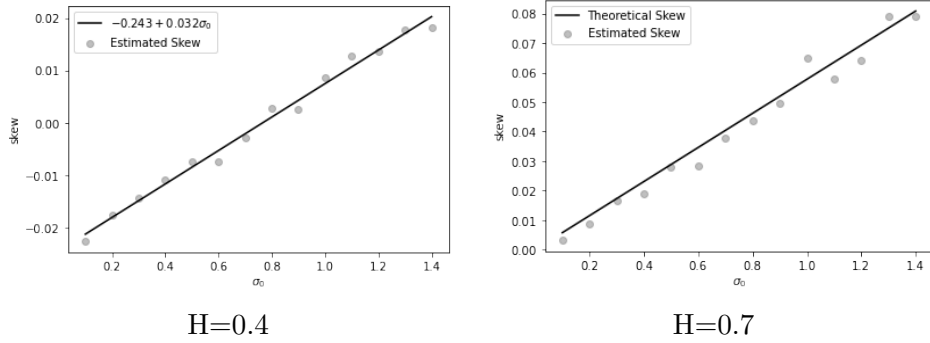


Figure 5: At-the-money IV skew as a function of  $\sigma_0$  under fractional Bergomi model

In particular,

$$\mathbb{E}(D_r \sigma(S_u)) = \mathbb{E}(\sigma'(S_u) \sigma(S_r) S_r).$$

This can be written as

$$\begin{aligned} \mathbb{E}(D_r \sigma(S_u)) &= \sigma'(S_0) \sigma(S_0) S_0 + \mathbb{E}((\sigma'(S_u) - \sigma'(S_0)) \sigma(S_r) S_r) \\ &\quad + \sigma'(S_0) \mathbb{E}((\sigma(S_r) - \sigma(S_0)) S_r). \end{aligned}$$

Then, using the mean value theorem and the fact that  $S_t$  has Hölder continuous sample paths of any order  $\gamma < \frac{1}{2}$ , we see that the last two terms of the last display will not contribute in the limit (12). Thus, (12) gives

$$\lim_{T \rightarrow 0} \partial_k I(0, k^*) = \frac{\sqrt{3}}{5} S_0 \sigma'(S_0) + \frac{\sqrt{3} \sigma(S_0)}{30},$$

which is the same as in (35). This serves as one more evidence of the validity of Theorem 1.

## 5.5 Approximations for the Asian call price

In this last section we study numerically the adequacy of the linear approximation of the price of an Asian call option given in equation (14) in the case of the SABR and fractional Bergomi models.

We start considering the SABR model and we proceed with the following numerical experiment. We randomly sample the parameters as  $\sigma_0 \sim U(0.2, 0.8)$ ,  $\alpha \sim U(0.3, 1.5)$  and  $\rho \sim U(-0.9, 0.9)$ , where  $U$  stands for the uniform distribution. We fix  $S_0 = 100$  and consider the following strikes  $K = (90, 95, \dots, 125)$  and maturities  $T = (0.01, 0.1, 0.5, 1, 2)$ . We then price the Asian call option using Monte Carlo with 100000 paths and discretization step 0.01 and then estimate the IV following the same approach as in Section 5.3. The approximation accuracy of the Monte Carlo for the IV is computed using the pointwise relative error with respect to the 95% Monte Carlo confidence interval and is presented in Table 1. We observe a high error in the case of short maturity deep OTM options with strike price equal to 120 and 125, which comes from the fact that in this region the price of the option is close to zero.

We then compare the estimated IV with the approximation formula (14). We compute in Table 2 the median relative percentage error, the 90% quantile and the maximum of the relative percentage error of the Monte Carlo prices computed across 2000 random parameter combinations. We consider the 90% quantile in order to take into account the fact that we might generate 'bad' parameter combinations that may require more Monte Carlo samples to converge. In order to help the visualization of these quantities we also

Maturity/Strike	90	95	100	105	110	115	120	125
0.01	6.78	1.41	0.97	1.09	2.41	6.69	104.39	105.01
0.10	1.58	1.18	1.07	1.00	1.04	1.16	1.36	1.66
0.50	1.82	1.16	1.02	0.97	1.08	1.41	1.91	2.74
1.00	2.07	1.85	1.72	1.64	1.60	1.59	1.61	1.68
2.00	3.26	3.20	3.02	2.94	2.87	2.87	2.90	2.92

Table 1: Median percentage error wrt the 95% Monte Carlo confidence interval for the SABR model.

plot the heat map in Figure 6. We see that the suggested formula works the best for short dated options with strikes close to ATM level. As we increase the maturity the quality of the approximation decreases and the error can be very big.

Maturity/Strike	90	95	100	105	110	115	120	125
0.01	4.07	0.40	0.24	0.28	0.55	1.19	2.93	5.44
0.10	0.78	0.46	0.34	0.40	0.56	0.88	1.29	1.79
0.50	215.50	216.26	216.60	216.12	215.27	214.31	213.39	212.64
1.00	2.79	2.43	2.27	2.38	2.59	2.89	3.36	3.78
2.00	4.48	4.10	3.89	3.86	4.02	4.33	4.81	5.27

(a) Median % error

Maturity/Strike	90	95	100	105	110	115	120	125
0.01	44.91	3.26	0.54	0.93	2.70	5.29	8.86	13.68
0.10	2.92	1.21	0.83	1.08	2.17	4.11	6.06	7.57
0.50	218.84	218.10	217.96	217.62	217.44	217.55	217.98	218.51
1.00	9.42	7.32	6.57	6.78	7.79	9.40	11.94	14.46
2.00	23.59	25.77	23.06	21.91	20.77	20.66	22.77	26.60

(b) 90th quantile % Error

Maturity/Strike	90	95	100	105	110	115	120	125
0.01	76.99	41.51	1.05	12.17	22.30	21.32	21.78	20.80
0.10	41.89	3.72	1.66	3.78	10.02	19.88	31.79	30.65
0.50	273.69	224.61	219.46	219.52	223.80	280.83	249.04	280.53
1.00	123.43	88.31	87.24	86.28	85.40	84.61	83.87	83.20
2.00	572.53	989.85	328.54	254.77	217.17	194.01	178.21	166.72

(c) Maximum % error

Table 2: Approximation error under the SABR model.

We finally plot an implied volatility surface for different maturities in Figure 7 to see the typical shape of the IV under the SABR model. We see that that the level of the implied volatility even for ATM options can shift considerably as we increase the maturity and is not necessarily linear.

Overall, we conclude that the suggested approximation formula is stable for short maturities and not too deep out and in-the-money options. Outside of these regions the quality of the approximation highly depends on the parameters of the model.

In the case of the fractional Bergomi model we randomly sample the parameters of the model as  $\sigma_0 \sim U(0.2, 0.8)$ ,  $v \sim U(0.3, 1.5)$  and  $\rho \sim U(-0.9, 0.9)$ . We fix  $S_0 = 100$

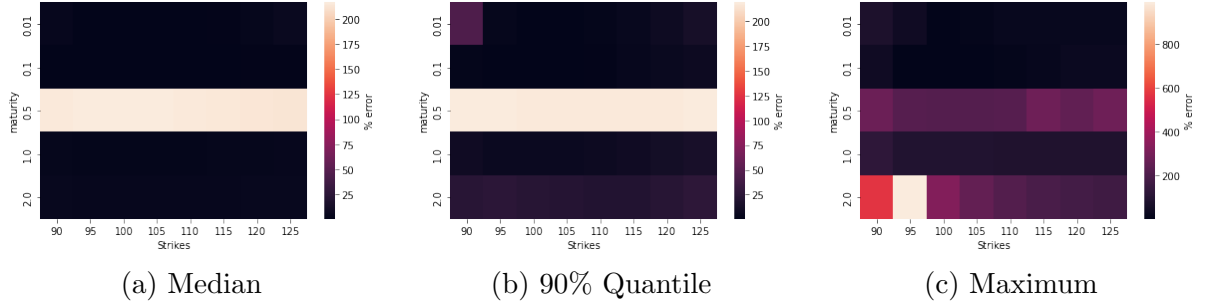


Figure 6: Accuracy of the approximation (14) under the SABR model.

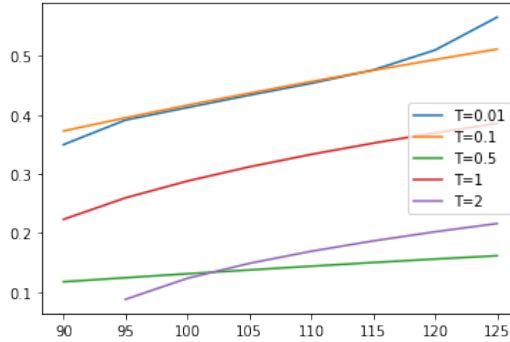


Figure 7: Typical surface of the IV under the SABR model.

and consider the strikes  $K = (90, 95, \dots, 125)$  and maturities  $T = (0.01, 0.1, 0.5, 1, 2)$ . In order to investigate the influence of roughness of the volatility process we consider two values of  $H = \{0.2, 0.7\}$ . We price the Asian call option using Monte Carlo with 100000 paths and discretization step 0.01.

We start with the case  $H = 0.2$ . The approximation accuracy of the Monte Carlo for the implied volatility is computed using the corresponding pointwise median relative error with respect to the 95% Monte Carlo confidence interval and is presented at Table 3.

Maturity/Strike	90	95	100	105	110	115	120	125
0.01	5.10	1.41	0.99	1.12	2.35	4.58	9.60	10.95
0.10	1.47	1.18	1.09	1.03	1.08	1.22	1.48	1.79
0.50	1.55	1.41	1.32	1.26	1.23	1.24	1.28	1.35
1.00	1.77	1.64	1.55	1.48	1.44	1.43	1.44	1.46
2.00	2.25	2.11	2.01	1.93	1.89	1.86	1.84	1.86

Table 3: Median percentage error wrt the 95% Monte Carlo confidence interval of fractional Bergomi model with  $H=0.2$ .

As for the SABR model, we compute the median relative percentage error, the 90% quantile and the maximum of relative percentage error across 1000 random parameter combinations in Table 4. The heat map is presented in Figure 8. We observe that the approximation works better for ATM options with short maturities. Additionally, we conclude that it exhibits an adequate performance in the range of 5% around the ATM strike for short dated options and quite a wide range of strikes for longer dated options.

As for the SABR model we plot in Figure 9 an IV surface for different maturities. We observe a considerable curvature for short maturity that smooths around the ATM

Maturity/Strike	90	95	100	105	110	115	120	125
0.01	11.00	5.29	0.69	4.85	7.22	7.75	9.62	18.76
0.10	5.57	2.80	1.34	2.53	5.09	6.94	8.34	9.49
0.50	3.74	2.37	2.34	1.98	2.91	4.42	6.00	7.23
1.00	3.49	2.96	3.16	2.80	2.88	3.64	4.73	5.85
2.00	4.28	4.25	4.30	4.13	3.91	4.03	4.47	5.03

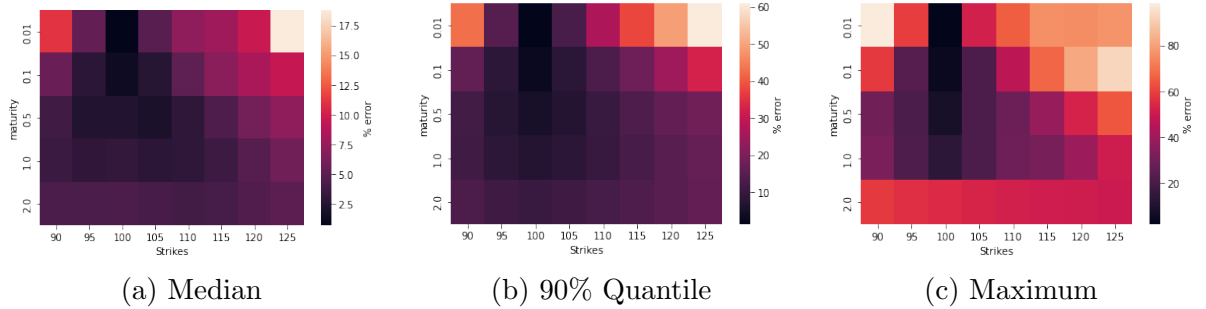
(a) Median % error

Maturity/Strike	90	95	100	105	110	115	120	125
0.01	42.98	14.75	1.33	12.96	26.83	38.08	49.11	60.95
0.10	16.39	8.49	2.80	7.91	13.38	18.16	25.08	32.56
0.50	11.84	7.48	5.26	7.05	10.40	13.58	16.56	18.68
1.00	11.40	8.38	7.04	8.10	10.16	12.59	14.96	17.09
2.00	13.28	11.26	10.33	11.19	12.35	13.51	15.30	16.68

(b) 90th quantile % error

Maturity/Strike	90	95	100	105	110	115	120	125
0.01	98.23	59.44	2.09	52.10	65.76	75.87	75.35	76.91
0.10	58.45	23.72	4.64	21.61	47.06	67.19	81.64	92.92
0.50	29.69	21.12	8.32	21.27	28.43	38.44	52.83	64.23
1.00	31.82	21.64	13.38	21.38	29.45	31.21	39.36	50.72
2.00	58.74	56.54	54.71	53.23	52.07	51.19	50.55	50.12

(c) Maximum % error

Table 4: The Approximation error of the IV under fractional Bergomi model with  $H=0.2$ .Figure 8: Accuracy of the approximation (14) under fractional Bergomi with  $H = 0.2$ .

values leading to the improvement in the behaviour of our approximation as maturity increases. This shape heavily depends on the parameters of the model, however this conclusion holds on average for our sample.

Finally, we follow the same approach the fractional Bergomi model with  $H=0.7$ . See Tables 5 and 6 and Figure 10. One can see that the behaviour of the errors is much better than in the case of  $H = 0.2$ . In general, the magnitudes of the errors turn out to be smaller. The approximation defined in equation (14) works quite well for a wide range of strikes and maturities. This fact is explained by the typical shape of the implied volatility of the considered model which is presented in Figure 11. We see that the curvature looks negligible as we increase the maturity of the option which makes linear approximation quite reasonable.

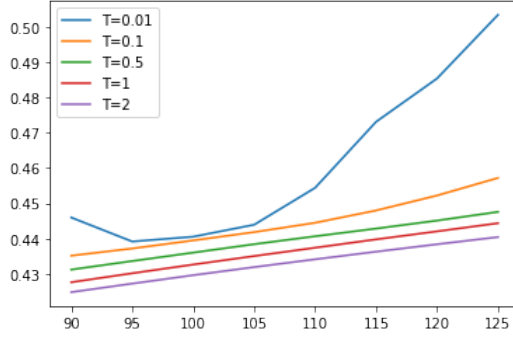


Figure 9: Typical surface of the IV under the fractional Bergomi model with  $H = 0.2$ .

Maturity/Strike	90	95	100	105	110	115	120	125
0.01	5.52	1.34	0.97	1.07	2.46	6.41	104.51	105.28
0.10	1.36	1.12	1.06	0.98	1.00	1.07	1.30	1.62
0.50	1.44	1.32	1.24	1.17	1.13	1.13	1.15	1.19
1.00	1.65	1.53	1.45	1.38	1.34	1.32	1.32	1.34
2.00	2.27	2.13	2.03	1.96	1.91	1.89	1.88	1.88

Table 5: Median percentage error wrt the 95% Monte Carlo confidence interval of fractional Bergomi model with  $H=0.7$ .

In conclusion, the behaviour of the approximation (14) heavily depends on the model. For OTM and ITM options the quality gets better with the decrease in the curvature of the implied volatility surface. For ATM options, the quality of the approximation and behaviour are quite stable for the considered models and reasonably impairs with the increase of the maturity.

Maturity/Strike	90	95	100	105	110	115	120	125
0.01	2.58	0.40	0.27	0.32	0.51	1.11	2.84	10.22
0.10	0.40	0.35	0.35	0.33	0.30	0.31	0.33	0.40
0.50	0.78	0.86	0.87	0.81	0.71	0.65	0.60	0.57
1.00	1.65	1.77	1.78	1.72	1.59	1.33	1.20	1.13
2.00	3.94	4.06	4.07	4.00	3.81	3.54	3.16	2.78

(a) Median % error

Maturity/Strike	90	95	100	105	110	115	120	125
0.01	39.71	1.64	0.59	0.90	2.38	3.77	7.59	12.34
0.10	0.88	0.71	0.67	0.63	0.64	0.84	1.89	2.35
0.50	1.61	1.64	1.62	1.58	1.46	1.37	1.40	1.75
1.00	3.53	3.59	3.59	3.51	3.36	3.11	2.90	2.95
2.00	10.16	10.07	10.02	9.89	9.61	9.34	9.05	8.75

(b) 90th quantile % error

Maturity/Strike	90	95	100	105	110	115	120	125
0.01	57.59	16.07	1.10	15.35	28.43	30.11	15.95	18.70
0.10	3.68	1.18	1.09	1.05	2.96	6.83	11.84	18.08
0.50	2.71	2.65	2.60	2.52	2.45	2.35	6.40	11.29
1.00	7.81	7.58	7.39	7.24	7.12	7.00	6.87	8.77
2.00	77.63	76.58	75.66	74.85	74.14	73.52	72.98	72.51

(c) Maximum % Error

Table 6: Approximation error of the IV under fractional Bergomi model with  $H=0.7$ .

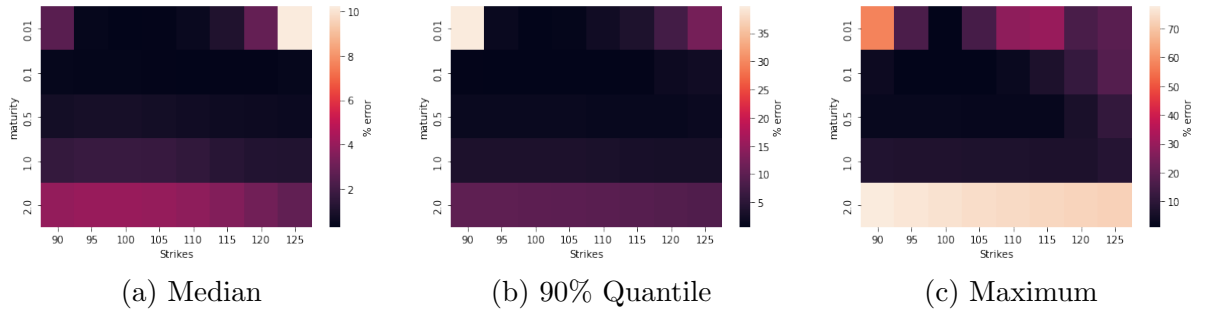


Figure 10: Accuracy of the approximation (14) under fractional Bergomi with  $H = 0.7$ .

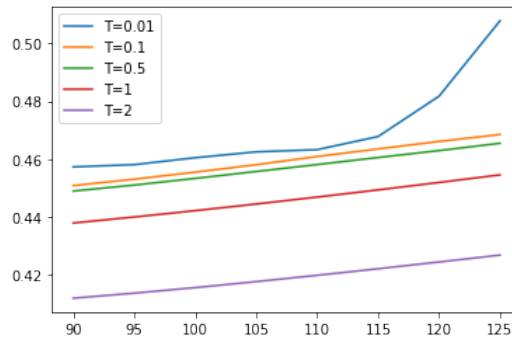


Figure 11: Typical surface of the IV under fractional Bergomi model with  $H = 0.7$ .

## A Computation of Malliavin derivatives

In this section we provide the computations of the first and second Malliavin derivatives of the processes  $S_t$ ,  $M_t$  and  $\phi_t$  defined in Section 2.

Using the fact that  $\sigma_t$  is adapted to the filtration of  $W'$  and the formula for the derivative of a stochastic integral (see for example (3.6) in Nualart and Nualart [13]), we get that, for  $0 \leq s \leq r \leq T$ ,

$$\begin{aligned} D_s^{W'} S_r &= S_r \left( \rho \sigma_s - \frac{1}{2} \int_s^r D_s^{W'} \sigma_u^2 du + \int_s^r D_s^{W'} \sigma_u dW_u \right), \\ D_s^B S_r &= S_r \sigma_s \sqrt{1 - \rho^2}, \\ D_s^{W'} M_r &= \frac{\rho \sigma_s S_s (T - s)}{T} + \int_s^r \frac{(T - u) D_s^{W'} (\sigma_u S_u)}{T} dW_u, \\ D_s^B M_r &= \frac{\sqrt{1 - \rho^2} \sigma_s S_s (T - s)}{T} + \int_s^r \frac{(T - u) \sigma_u D_s^B (S_u)}{T} dW_u. \end{aligned}$$

Moreover, appealing to (8), we find that

$$\begin{aligned} D_s^W S_r &= \rho S_r \left( -\frac{1}{2} \int_s^r D_s^{W'} \sigma_u^2 du + \int_s^r D_s^{W'} \sigma_u dW_u \right) + S_r \sigma_s, \\ D_s^W M_r &= \frac{\sigma_s S_s (T - s)}{T} + \rho \int_s^r \frac{(T - u) D_s^{W'} (\sigma_u S_u)}{T} dW_u \\ &\quad + \sqrt{1 - \rho^2} \int_s^r \frac{(T - u) D_s^B (\sigma_u S_u)}{T} dW_u. \end{aligned}$$

Finally, from the definition of  $\phi_t$ , we conclude that

$$\begin{aligned} D_s^W \phi_r &= \frac{\rho(T - r) D_s^{W'} (\sigma_r S_r)}{T M_r} - \frac{\rho(T - r) S_r \sigma_r D_s^{W'} M_r}{T M_r^2} \\ &\quad + \frac{\sqrt{1 - \rho^2} (T - r) D_s^B (\sigma_r S_r)}{T M_r} - \frac{\sqrt{1 - \rho^2} (T - r) S_r \sigma_r D_s^B M_r}{T M_r^2}. \end{aligned} \tag{36}$$

We next compute the second Malliavin derivatives. Similarly as before, using the fact that we can differentiate Lebesgue integrals of stochastic processes (see for example

Proposition 3.4.3 in Nualart and Nualart [13]), we get that, for  $0 \leq s \leq r \leq u \leq T$ ,

$$\begin{aligned}
D_s^B D_r^{W'} S_u &= S_u \sigma_s \sqrt{1 - \rho^2} \left( \rho \sigma_r - \frac{1}{2} \int_r^u D_r^{W'} \sigma_v^2 dv + \int_r^u D_r^{W'} \sigma_v dW_v \right), \\
D_s^{W'} D_r^{W'} S_u &= S_u \left( \rho \sigma_s - \frac{1}{2} \int_s^u D_s^{W'} \sigma_v^2 dv + \int_s^u D_s^{W'} \sigma_v dW_v \right) \\
&\quad \times \left( \rho \sigma_r - \frac{1}{2} \int_r^u D_r^{W'} \sigma_v^2 dv + \int_r^u D_r^{W'} \sigma_v dW_v \right) \\
&\quad + S_u \left( \rho D_s^{W'} \sigma_r - \frac{1}{2} \int_r^u D_s^{W'} D_r^{W'} \sigma_v^2 dv + \int_r^u D_s^{W'} D_r^{W'} \sigma_v dW_v \right), \\
D_s^{W'} D_r^B S_u &= \sqrt{1 - \rho^2} S_u D_s^{W'} \sigma_r + \sqrt{1 - \rho^2} \sigma_r D_s^{W'} S_u, \\
D_s^{W'} D_r^{W'} M_u &= \frac{\rho(T - r) D_s^{W'} (\sigma_r S_r)}{T} + \int_r^u \frac{(T - v) D_s^{W'} D_r^{W'} (\sigma_v S_v)}{T} dW_v, \\
D_s^B D_r^{W'} M_u &= \frac{\rho(T - r) \sigma_r D_s^B S_r}{T} + \int_r^u \frac{(T - v) D_s^B D_r^{W'} (\sigma_v S_v)}{T} dW_v, \\
D_s^{W'} D_r^B M_u &= \frac{\sqrt{1 - \rho^2} (T - r) D_s^{W'} (\sigma_r S_r)}{T} + \int_r^u \frac{(T - v) D_s^{W'} (\sigma_v D_s^B S_v)}{T} dW_v, \\
D_s^B D_r^B M_u &= \frac{\sqrt{1 - \rho^2} (T - r) \sigma_r D_s^B (S_r)}{T} + \int_r^u \frac{(T - v) \sigma_v D_s^B D_r^B S_v}{T} dW_v,
\end{aligned} \tag{37}$$

and

$$\begin{aligned}
D_s^W D_r^W \phi_u &= \frac{\rho^2 (T - u) D_s^{W'} D_r^{W'} (\sigma_u S_u)}{T M_u} - \frac{\rho^2 (T - u) D_s^{W'} (\sigma_u S_u) D_s^{W'} M_u}{T M_u^2} \\
&\quad - \frac{\rho^2 (T - u) D_s^{W'} (\sigma_u S_u D_r^{W'} M_u)}{T M_u^2} + \frac{2\rho^2 (T - u) \sigma_u S_u D_s^{W'} M_u D_r^{W'} M_u}{T M_u^3} \\
&\quad + \frac{\rho \sqrt{1 - \rho^2} (T - u) D_s^{W'} D_r^B (\sigma_u S_u)}{T M_u} - \frac{\rho \sqrt{1 - \rho^2} (T - u) D_r^B (\sigma_u S_u) D_s^{W'} M_u}{T M_u^2} \\
&\quad - \frac{\rho \sqrt{1 - \rho^2} (T - u) D_s^{W'} (\sigma_u S_u D_r^B M_u)}{T M_u^2} + \frac{2\rho \sqrt{1 - \rho^2} (T - u) \sigma_u S_u D_r^B M_u D_s^{W'} M_u}{T M_u^3} \\
&\quad + \frac{\rho \sqrt{1 - \rho^2} (T - u) D_s^B D_r^{W'} (\sigma_u S_u)}{T M_u} - \frac{\rho \sqrt{1 - \rho^2} (T - u) D_r^{W'} (\sigma_u S_u) D_s^B M_u}{T M_u^2} \\
&\quad - \frac{\rho \sqrt{1 - \rho^2} (T - u) D_s^B (\sigma_u S_u D_r^{W'} M_u)}{T M_u^2} + \frac{\rho \sqrt{1 - \rho^2} (T - u) \sigma_u S_u D_r^{W'} M_u D_s^B M_u}{T M_u^3} \\
&\quad + \frac{(1 - \rho^2) (T - u) D_s^B D_r^B (\sigma_u S_u)}{T M_u} - \frac{(1 - \rho^2) (T - u) D_r^B (\sigma_u S_u) D_s^B M_u}{T M_u^2} \\
&\quad - \frac{(1 - \rho^2) (T - u) D_s^B (S_u \sigma_u D_r^B M_u)}{T M_u^2} + \frac{2(1 - \rho^2) (T - u) S_u \sigma_u D_r^B M_u D_s^B M_u}{T M_u^3}.
\end{aligned} \tag{38}$$

## References

- [1] Alòs, E. (2006). A generalization of the Hull and White formula with applications to option pricing approximation, *Finance and Stochastics* 10, 353–365.
- [2] Alòs, E. and León, J. A. and Vives, J. (2007). On the short-time behavior of the implied volatility for jump-diffusion models with stochastic volatility, *Finance and Stochastics* 11, 373–399.

- [3] Alòs, E. and León, J. A. (2017). On the curvature of the smile in stochastic volatility models, *SIAM Journal on Financial Mathematics* 8, 373–399.
- [4] Alòs, E. and León, J. A. (2019). A note on the implied volatility for floating strike Asian options, *Decisions in Economics and Finance* 42, 743–758.
- [5] Alòs, E. and Shiraya, J. A. (2019). Estimating the Hurst parameter from short term volatility swaps: a Malliavin calculus approach, *Finance and Stochastics* 23, 423–447.
- [6] Alòs, E. and García-Lorite, D. (2021). Malliavin Calculus in Finance. Chapman and Hall/CRC.
- [7] Alòs, E. and García-Lorite, D. and Muguruza, A. (2022). On smile properties of volatility derivatives: understanding the VIX skew, *SIAM Journal on Financial Mathematics* 13, 32–69.
- [8] Chatterjee, R., Cui, Z., Fan, J. and Liu, M. (2018) An efficient and stable method for short maturity Asian options, *J. Futures Markets* 38, 1470—1486.
- [9] Forde, M. and Jacquier, A. (2010). Robust Approximations for Pricing Asian Options and Volatility Swaps Under Stochastic Volatility, *Applied Mathematical Finance* 17, 241–259.
- [10] Fouque, J.-P. and Han, C.-H. (2003). Pricing Asian options with stochastic volatility, *Quantitative Finance* 3, 353–362.
- [11] Jäckel, P. (2015). Let’s be rational, *Wilmott* 75, 40–53.
- [12] Lee, R.W. (2005). Implied Volatility: Statics, Dynamics, and Probabilistic Interpretation. In: Baeza-Yates, R., Glaz, J., Gzyl, H., Hüslér, J., Palacios, J.L. (eds) Recent Advances in Applied Probability. Springer, Boston, MA.
- [13] Nualart, D. and Nualart, E. (2018). Introduction to Malliavin Calculus. Cambridge University Press.
- [14] Pirjol, D. and Zhu, L. (2016). Short maturity Asian options in local volatility models, *SIAM Journal on Financial Mathematics* 7, 947–992.
- [15] Pirjol, D. and Zhu, L. (2019). Short maturity Asian options in the CEV model, *Probability in the Engineering and Informational Sciences* 33, 258–290.
- [16] Yang, Z. and Ewald, C.-O. (2009). Implied volatility from Asian options via Monte Carlo methods, *International Journal of Theoretical and Applied Finance* 12, 153–178.